Citation: Cell Death and Disease (2011) 2, e224; doi:10.1038/cddis.2011.105
© 2011 Macmillan Publishers Limited All rights reserved 2041-4889/11
www.nature.com/cddis

Temporal blastemal cell gene expression analysis in the kidney reveals new Wnt and related signaling pathway genes to be essential for Wilms' tumor onset

M Maschietto[1], AP Trapé[1,2], FS Piccoli[1], TI Ricca[1], AAM Dias[3], RA Coudry[4], PA Galante[5], C Torres[6], L Fahhan[7], S Lourenço[4], PE Grundy[8], B de Camargo[9], S de Souza[5], EJ Neves[7], FA Soares[4], H Brentani[10] and DM Carraro*[,1]

Wilms' tumors (WTs) originate from metanephric blastema cells that are unable to complete differentiation, resulting in triphasic tumors composed of epithelial, stromal and blastemal cells, with the latter harboring molecular characteristics similar to those of the earliest kidney development stages. Precise regulation of Wnt and related signaling pathways has been shown to be crucial for correct kidney differentiation. In this study, the gene expression profile of Wnt and related pathways was assessed in laser-microdissected blastemal cells in WTs and differentiated kidneys, in human and in four temporal kidney differentiation stages (i.e. E15.5, E17.5, P1.5 and P7.5) in mice, using an orthologous cDNA microarray platform. A signaling pathway-based gene signature was shared between cells of WT and of earliest kidney differentiation stages, revealing genes involved in the interruption of blastemal cell differentiation in WT. Reverse transcription-quantitative PCR showed high robustness of the microarray data demonstrating 75 and 56% agreement in the initial and independent sample sets, respectively. The protein expression of CRABP2, IGF2, GRK7, TESK1, HDGF, WNT5B, FZD2 and TIMP3 was characterized in WTs and in a panel of human fetal kidneys displaying remarkable aspects of differentiation, which was recapitulated in the tumor. Taken together, this study reveals new genes candidate for triggering WT onset and for therapeutic treatment targets.
Cell Death and Disease (2011) **2,** e224; doi:10.1038/cddis.2011.105; published online 3 November 2011
Subject Category: Cancer

Conserved mechanisms that underlie the relationship between normal development and tumorigenesis may give insights into the earliest events that drive transformation. Normal kidney differentiation requires a fine regulation of morphogenetic events, and its deregulation may lead to kidney abnormalities, including agenesis, dysplasia, hypoplasia and tumors.[1] Wilms' tumor (WT), or nephroblastoma, arises from metanephric blastemal cells that are unable to complete the mesenchymal–epithelial transition (MET) resulting in a tumor with varying proportions of undifferentiated blastemal and stromal cells and primitive epithelial structures. These histological features resemble fetal kidneys (FKs) and make WT a model for morphological recapitulation of the earliest kidney developmental stages.[1,2]

Additional evidence for recapitulation of the earliest kidney differentiation stages in WT has been provided by molecular studies, exemplified by the *WT1*, *IGF2* and other genes, implicated in nephrogenesis and associated with Wilms' tumorigenesis.[2,3] A high degree of similarity has also been detected in gene expression profiles of the earliest kidney differentiation stages and whole WT.[4,5] More recently, we have provided evidence that, among the three histological WT components, blastemal cells display a gene expression profile similar to that found in the initial stages of nephrogenesis, suggesting that the blastemal component, and not the whole tumor, preserves the molecular events involved in WT onset.[6]

Kidney differentiation involves complex interactions between epithelial and mesenchymal cells, and signal transduction pathways have a fundamental role in controlling cell–cell interactions. The Wnt signaling pathway, an interrelated pathway with key roles in embryogenesis and cancer, consists of two highly connected main branches, namely the *CTNNB1*-dependent and the *CTNNB1*-independent Wnt pathways. The *CTNNB1*-dependent pathway is essential for controlling embryonic development and adult cell homeostasis. β-Catenin, encoded by *CTNNB1*, functions as coactivator of the TCF/LEF family of transcription factors during embryonic development and is a key component of cell–cell

[1]Laboratory of Genomics and Molecular Biology, CIPE—AC Camargo Hospital, São Paulo, SP, Brasil; [2]Departamento de Radiologia e Oncologia—Faculdade de Medicina da Universidade de São Paulo (FMUSP), São Paulo, SP, Brasil; [3]Laboratory of Experimental Genetics, Department of General Biology—Universidade Federal de Minas Gerais, Belo Horizonte, MG, Brasil; [4]Department of Anatomic Pathology—AC Camargo Hospital, São Paulo, SP, Brasil; [5]Laboratory of Bioinformatics—Ludwig Institute for Cancer Research, São Paulo, SP, Brasil; [6]Laboratory of Bioinformatics, CIPE—AC Camargo Hospital, São Paulo, SP, Brasil; [7]Instituto de Matemática e Estatística da Universidade de São Paulo (IME-USP), São Paulo, SP, Brasil; [8]Pediatric Hematology, Oncology and Palliative Care—Stollery Children's Hospital, Edmonton, Alberta, Canada; [9]Research Pediatric Hematology-Oncology Program, Instituto Nacional do Câncer, Rio de Janeiro, RJ, Brasil and [10]Departamento de Psiquiatria—Faculdade de Medicina da Universidade de São Paulo (FMUSP), São Paulo, SP, Brasil
*Corresponding author: DM Carraro, Laboratory of Genomics and Molecular Biology, Rua Prof. Antonio Prudente, 109—1° andar, CIPE—Hospital A.C. Camargo, CEP 01509-010 São Paulo, SP, Brasil. Tel: +55 11 2189 5023; Fax: +55 11 2189 5185; E-mail: dirce.carraro@cipe.accamargo.org.br
Keywords: Wilms' tumor; blastemal component; Wnt signaling pathway; kidney development; gene expression
Abbreviations: ACIS, Automated Cellular Imaging System III; aRNA, amplified RNA; DK, differentiated kidney; FFPE, formalin-fixed, paraffin-embedded; FK, fetal kidney; hcrHMs, conserved regions of human and mouse orthologs; HM, human and mouse; MET, mesenchymal–epithelial transition; RT-qPCR, reverse transcription-quantitative PCR; TMA, tissue microarray; WT, Wilms' tumor
Received 13.6.11; revised 26.8.11; accepted 21.9.11; Edited by M Federici

adhesion complexes in differentiated cells. Wnt ligands activate the *CTNNB1*-dependent pathway, leading to nuclear accumulation of β-catenin, which acts as a coactivator for transcription factors. In the absence of Wnt ligands, this pathway is inactivated by a destruction complex that phosphorylates β-catenin, leading to ubiquitination, proteasomal degradation and prevention of β-catenin accumulation in the nucleus.[7] Therefore, nuclear accumulation of β-catenin is an indirect marker for pathway activation and has been observed in WT.[8–10] *APC*, a component of the β-catenin destruction complex, is also found in the nucleus of blastemal cells in the earliest embryonic kidney stages and in WT.[6] The *CTNNB1*-independent Wnt pathway comprises two segments, namely the planar cell polarity and calcium signaling segments,[11] and its proper regulation has also been considered important in maintaining correct cell differentiation in the kidney. The calcium signaling components *PLCG2*[6] and *WNT5A*[12] are downregulated in WT, and their fine regulation seems to have an important role in kidney differentiation.

The strong connection between nephrogenesis and WT highlights the importance of characterizing gene expression modulation in the Wnt and related signaling pathways. Identification of genes expressed during kidney differentiation arrest may be necessary to determine the earliest alterations that drive WT onset and, consequently, are potential molecular markers or therapeutic target candidates. In this study, we characterized gene expression patterns of the Wnt and related signaling pathways in blastemal cells in kidney developmental stages in mice and in WT in humans. For this purpose, we established a cross-species hybridization model to assess the gene expression modulation in both species on a cDNA platform. Our findings revealed 18 genes commonly regulated in the earliest kidney developmental stages and in WT. Expression patterns based on this gene set could discriminate blastemal WT cells and FK cells from those of differentiated kidneys (DKs) from both species. Detailed characterization of the protein expression of human FKs and WT revealed some interesting aspects of gene modulation in nephrogenesis and in WT. Overall, we revealed new genes that determine kidney differentiation arrest and are potential molecular markers or therapeutic target for WT patients.

Results

Evaluation of cross-species hybridization for the construction of a cDNA platform. To test the robustness of interspecific hybridizations, we interrogated 1334 sequences classified as highly conserved regions of human and mouse orthologous using RNA from kidney and liver of both species (see Material and Methods). Correlation between technical replicates and variance among the triplicate hybridization experiments were compared between interspecific (mouse RNA samples and human cDNA platform) and intraspecific (human RNA samples and human cDNA platform) hybridizations, with the latter considered the gold-standard experiment.

Technical replicates of interspecific hybridizations generated highly reproducible data, with Pearson's correlations ranging from 83 to 86% (average = 84.7%), similarly to intraspecific hybridizations, which resulted in 88–95% (average = 91.3%). To evaluate variance across the experiments, Levene's test was used to compare the fluorescence intensities of each spot in the intraspecific and interspecific hybridization replicates. For 90.6% of the spots (1195 out of 1334), the variability across the interspecific hybridizations was equal to or lower than that across the intraspecific hybridizations.

These analyses indicated that the criteria for defining highly similar orthologous sequences and the hybridization conditions resulted in robust interspecific hybridization data that were similar to data obtained for the intraspecific hybridizations.

Therefore, the same criteria for defining similar regions in the cDNA sequences (i.e. an *e*-value^{-5} and a minimum alignment of 50%) were used for constructing the orthologous cDNA platform used in this study. In total, 326 orthologous cDNA partial fragments with high similarity at the nucleotide level between human and mouse (HM) sequences were immobilized on a custom cDNA platform (Supplementary File 1) to assess gene expression regulation in both species.

Characterization of differentially expressed genes between WT and DK. From the 326 Wnt and related signaling pathway genes assessed in WT and DK, 47 were differentially expressed; and 18 and 29 were downregulated and upregulated in WT, respectively ($P<0.05$; Table 1).

Annotation of the biological processes classified the 47 differentially expressed genes into cell communication, development, organogenesis, morphogenesis, phosphorylation, regulation of transcription, transport and other categories without any detectable preferential distribution (Table 2).

Identification of genes involved in the earliest event that drives WT onset. To identify genes that recapitulate the expression profile of the earliest kidney developmental

Table 1 Differentially expressed genes between WT and DK

Downregulated genes in WT			Upregulated genes in WT			
CDC7	*ITPR3*	*VANGL2*	*COL5A1*	*CARKL*	*DMPK*	*PIK3C3*
CDH6	*MAPK9*	*WNT3*	*INPP5B*	*WNT5B*	*CRABP2*	*HDGF*
CDS1	*OCRL*	*WNT5B*	*EYA3*	*SFRP2*	*FRZB*	*PPP2R1A*
DVL2	*PIK3CA*		*LRP6*	*FZD2*	*GRK7*	*JUN*
EYA4	*PIK3CD*		*PIP5K2B*	*IGF1R*	*TESK1*	*IGF2*
FN3K	*PIP5K2C*		*PAX2*	*LRP1*	*TCF7L2*	
FRAT2	*TBL1XR1*		*PCTK2*	*FZD4*	*OFD1*	
HIPK1	*TIMP3*		*FZD10*	*CSNK2A1*	*RGS4*	

Table 2 Classification of differentially expressed genes between relapse and no-relapse WT samples within the biological process categories

Biological process categories	Upregulated genes in WT	Downregulated genes in WT
Cell communication	*INPP5B, PIP5K2B, RGS4*	*CDH6, CDS1, DVL2, FRAT2, PIK3CA, WNT3, WNT5B*
Development, organogeneis, morphogenesis	*EYA3, FRZB, FZD10, FZD2, FZD4, GRK7, IGF2, PAX2, PPP2R1A, SFRP2, WNT5B*	*EYA4, VANGL2*
Phosphorylation	*CSNK2A1, DMPK, IGF1R, PCTK2, PPP2R1A, TESK1*	*HIPK1, MAPK9, PIP5K2C, PIK3CD*
Regulation of transcription	*COL5A1, HDGF, JUN, TCF7L2*	—
Transport	*CRABP2, LRP1, PIK3C3*	*ITPR3*
Others	*CARKL, LRP6, OFD1*	*CDC7, FN3K, OCRL, TBL1XR1, TIMP3*

stages and consequently drive tumorigenesis in WT, genes downregulated and upregulated in WT, compared with DK, were compared with genes with increasing and decreasing behavior during kidney cell differentiation. The 326 genes were evaluated in 4 stages of mouse nephrogenesis, which represent the differentiation of metanephric blastema into fully DK cells, revealing 72 and 64 genes with increasing and decreasing expressions, respectively (Supplementary Figure 1). The others 190 genes presented diverse expression behavior during kidney cell differentiation and were not further analyzed.

Thus, the 72 increasing genes were compared with the 18 WT blastemal cell downregulated genes, and the 64 decreasing genes were compared with the 29 WT blastemal cell upregulated genes. This analysis revealed that 18 genes, 7 with increasing and 11 with decreasing expressions during mouse metanephric blastema cell differentiation (Figure 1a), were downregulated (*TIMP3*, *HIPK1*, *CDH6*, *ITPR3*, *FRAT2*, *PIK3CA* and *MAPK9)* and upregulated (*PAX2*, *FZD10*, *CARKL*, *WNT5B*, *FZD2*, *CRABP2*, *FRZB*, *GRK7*, *TESK1*, *HDGF* and *IGF2*) in WT blastemal compared with DK cells, respectively.

Hierarchical clustering based on the expression pattern of the 18 genes grouped differentiated and intermediate kidneys from humans and mice together and discriminated them from WT samples, which were grouped with the pool of human FKs and the earliest mouse embryonic kidneys (Figure 1b). This result revealed two important aspects of this study: the model for interspecific hybridization was appropriate for studying human tumorigenesis and mouse embryogenesis, and a gene expression signature linked to Wnt and related signaling pathways was associated with WT onset.

A high level of robustness was detected in this study, with 75% agreement between microarray and reverse transcription-quantitative PCR (RT-qPCR) experiments in the initial sample set. In total, 9 out of 12 genes displayed concordant expression. *CRABP2*, *HDGF*, *IGF2*, *PAX2*, *SHPK*, *TESK1* and *WNT5B* were upregulated and *HIPK1* and *TIMP3* were downregulated, in WT blastemal cells compared to DK glomerular cells (Figure 1c). Interestingly, hierarchical clustering based on the 12 genes assessed by RT-qPCR, independent of their validation, could discriminate DK from 100% of WT samples (Supplementary Figure 3) reinforcing the association of this gene signature with WT.

Evaluation of expression levels using a broader group of WT and DK samples. To assess the transcriptional difference of the 9 technically validated genes (*CRABP2*, *IGF2*, *PAX2*, *WNT5B*, *TIMP3*, *HIPK1*, *TESK1*, *SHPK* and *HDGF*) in samples with different biological backgrounds, we evaluated an independent group of 35 blastema-enriched WT and 13 cortex-enriched DK samples. The data from *CRABP2*, *HDGF*, *IGF2*, *TIMP3* and *WNT5B* agreed with the initial sample group. *HIPK1* did not satisfy the fold-change criteria ($\geq$3), despite showing statistical significance (Figure 2).

Characterization of protein expression in WT and during human kidney embryogenesis. First, correspondence between the mRNA and protein was evaluated based on the immunohistochemical labeling intensity of each protein in the blastemal WT and glomerular DK cells. Proteins encoded by 8 out of 18 genes were evaluated in 145 WT and 20 DKs. A high percentage of agreement was observed, with 5 out of 8 (62.5%) genes displaying the same expression tendency at mRNA and protein levels. *CRABP2*, *GRK7*, *HDGF*, *IGF2* and *TESK1* were overexpressed in WT. *WNT5B* and *FZD2* did not show a difference between WT and DK, and *TIMP3* had opposite results, that is, its mRNA was underexpressed in WT, and its protein product was overexpressed (Figure 3).

Second, protein positivity was characterized in embryonic kidneys, from undifferentiated mesenchymal metanephric to fully differentiated cells. In addition, WT and DK samples were classified as either negative or positive for each protein (Table 3).

A protein expression profile that recapitulated the earliest kidney developmental stages could be observed in WT for the majority of the eight assessed proteins (Figure 3).

Cytoplasmic and some nuclear CRABP2 positivity was detected in every cells undergoing MET after ureteric bud induction and before cells adopted an epithelial morphology. CRABP2 was not detected at any of the subsequent cell differentiation stages. The majority of WT samples displayed strong CRABP2 expression in the nucleus (107 out of 113 samples) and in the cytoplasm (101 out of 108 samples).

With regard to IGF2, cytoplasmic positivity was observed in all embryonic kidneys, with a slightly stronger positivity in the earliest stages. DK cells were considered IGF2 negative, and in WTs, IGF2 expression was observed in 96 out of 112 blastemal cells.

GRK7 was observed in the cytoplasm and in membranes of all embryonic kidneys, showing a slight decrease in the DK. In DK cells, half of the glomerular cells reported positive cytoplasm labeling, and the majority of cells also presented membrane positivity. All but one blastemal WT sample were positive for GRK7 in the cytoplasm (105 out of 106 samples) and in the membrane (116 out of 117 samples).

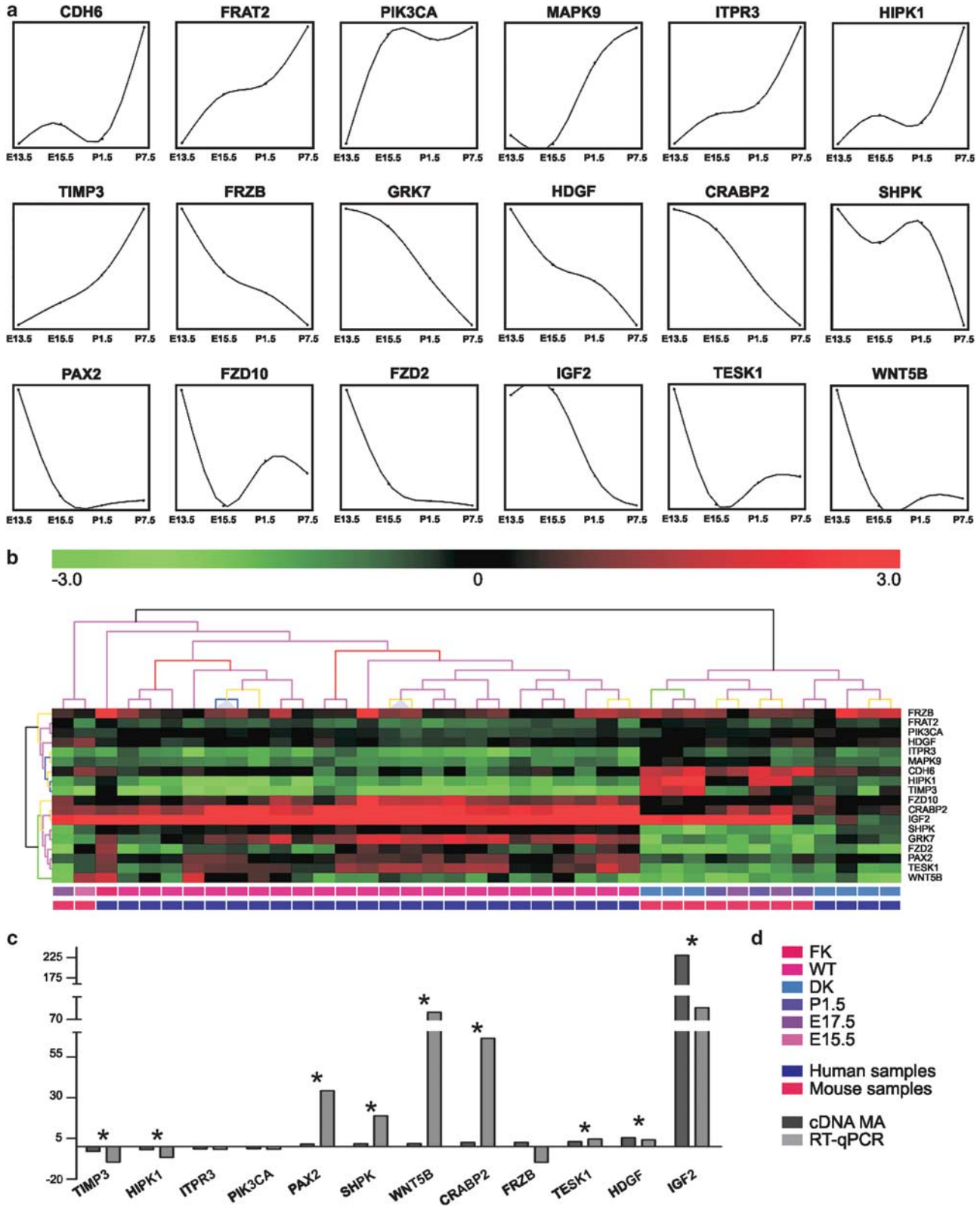

Figure 1 Wilms tumor signature set. (**a**) Expression behavior of the 18 genes during nephrogenesis in mouse. ↓ and ↑ indicate downregulation and upregulation in Wilms tumor, respectively, in comparison with differentiated kidney at transcriptional level. (**b**) Unsupervised hierarchical clustering based on expression pattern of the 18 genes. Black lines correspond to 90–100% of reliability assessed by Bootstrap. (**c**) Comparison of cDNA microarray and RT-qPCR experiments. (*) Represents differentially expressed genes assessed by RT-qPCR that fulfilled cutoff criteria (fold change >3 and $P<0.05$). (**d**) Legend of colors. FK, fetal kidney; WT, Wilms tumor; DK, differentiated kidney; P1.5, 1.5-day-old mouse kidney; E17.5 and E15.5, fetal kidney from 17.5 and 15.5-day-old mouse embryo, respectively

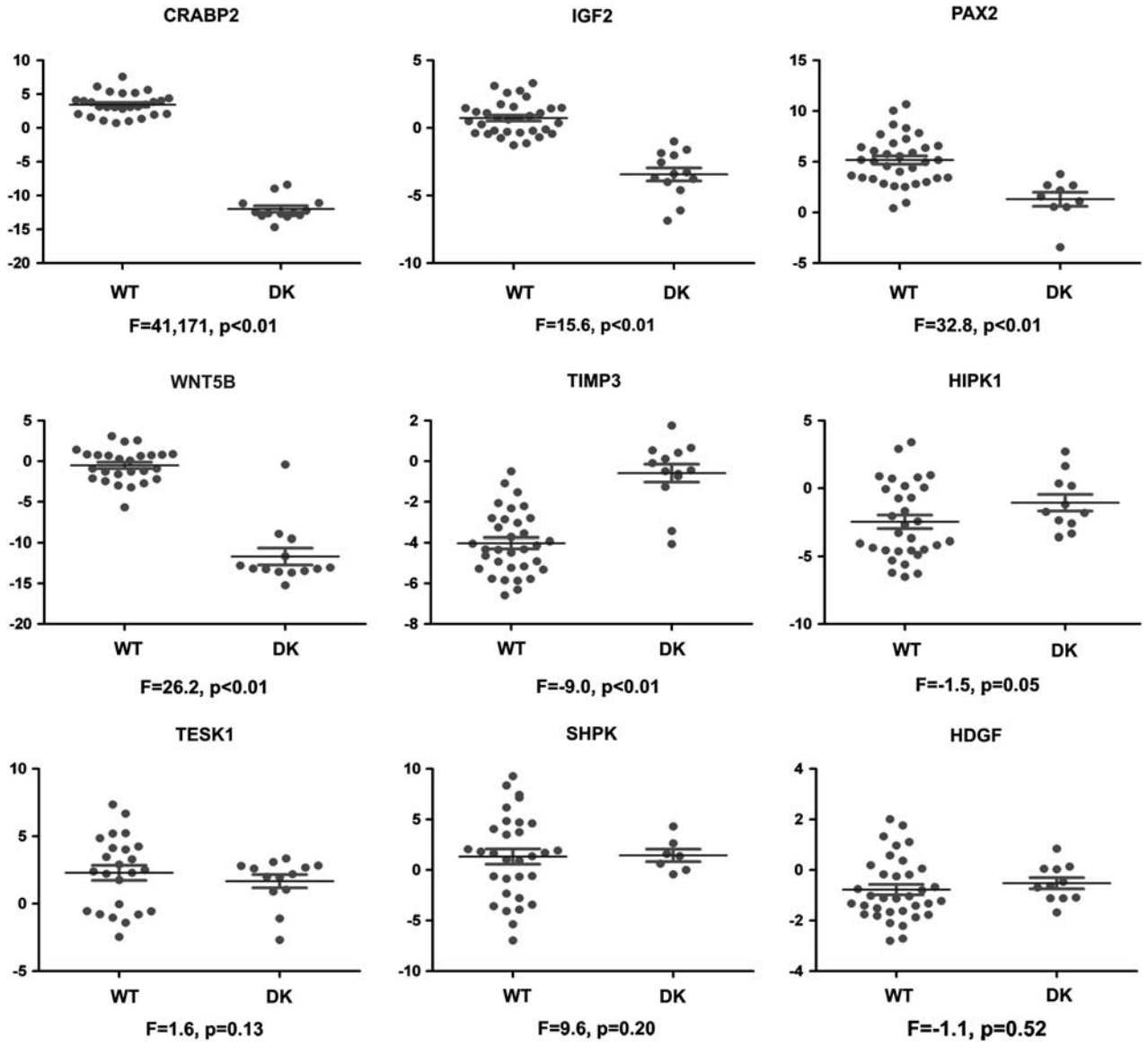

Figure 2 Biological evaluation of differentially expressed genes. Comparison of gene expression between Wilms tumor and differentiated kidney. WT: Wilms tumor; DK: differentiated kidney; F: fold change and *P*: *P*-value axis *Y*: Log2 relative expression. Negative and positive values correspond to downregulation and upregulation in WT, respectively. (*) Represents differentially expressed genes with fold change >3 and $P<0.05$

TESK1 exhibited a weak cytoplasmic positivity, primarily in tubular cells and a few embryonic kidney glomerular cells; in DKs, some glomerular cells were also positive. TESK1 showed positive staining in the cytoplasm of the majority of the WT blastemal components (110 out of 114 samples).

HDGF nuclear positivity was observed in some cells from all FK stages and DK. HDGF was positive in the cytoplasm of 56 out of 118 cells and in the nucleus of 52 out of 111 WT blastemal components.

TIMP3 was labeled in cell membranes and in the nuclei of embryonic kidney cells. TIMP3 was also observed in the cytoplasm and nucleus of DKs and in WT blastemal cells; however, stronger labeling was observed in the latter. Whereas the majority of samples were positive in the cytoplasm (101 out of 116 samples) less than half were positive in the nucleus (47 out of 111 samples).

In nephrogenesis, WNT5B was observed after renal vesicle formation, when cells are organizing to form kidney structures, such as glomeruli and tubules. WNT5B positivity was observed mainly in the apical cell membrane. In DK, WNT5B nuclear positivity was observed in some cells. In the WT blastemal component, WNT5B was observed in the cytoplasm in 8 out of 120 samples and in the membrane in 28 out of 113 samples.

With regard to FZD2, FKs were membrane positive in cell types ranging from undifferentiated metanephric blastema cells to differentiated glomerular and tubular cells. In WT blastemal cells, FZD2 was observed in the membrane in 37 out of 106 samples.

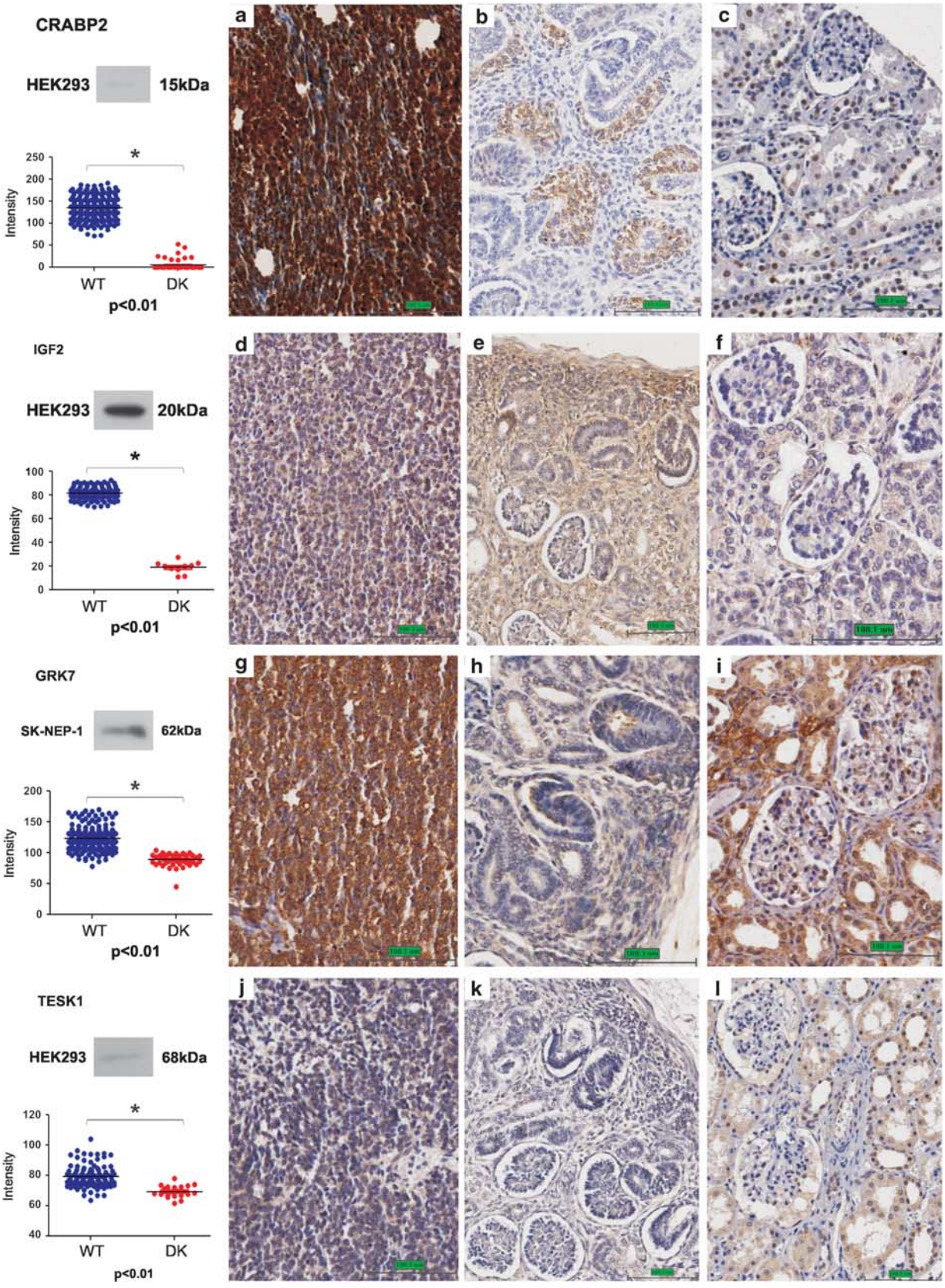
CRABP2
HEK293
15kDa
Intensity
WT
DK
p<0.01
IGF2
HEK293
20kDa
GRK7
SK-NEP-1
62kDa
TESK1
HEK293
68kDa
a
b
c
d
e
f
g
h
i
j
k
l

Assessment in relapse and no-relapse WT samples. To determine whether the 9 technically validated genes (i.e. *CRABP2*, *IGF2*, *PAX2*, *WNT5B*, *TIMP3*, *HIPK1*, *TESK1*, *SHPK* and *HDGF*) had a role in the latter events of WT progression, their expression levels were assessed in 35 blastemal-enriched WT samples that included 12 relapse and 23 no-relapse samples (Supplementary Figure 4). Only *IGF2* was differentially expressed ($P<0.01$); presenting downregulation in relapse WTs. *TESK1* was also downregulated in relapse WTs, but the *P*-value was borderline ($P=0.06$).

In addition, in an effort to find prognostic markers for WT, possible associations between protein expression (CRABP2, GRK7, HDGF, IGF2, TESK1, WNT5B, FZD2 and TIMP3) and clinicopathological variables (relapse, clinical stage, first treatment, number of drugs used, death, age of diagnosis and gender) were evaluated. No association was found, reinforcing that these molecular events had a role rather in tumorigenesis than in progression of WT.

Discussion

Embryonic tumors are intimately linked to embryogenesis, tissue growth and maturation process. Embryogenesis and tumorigenesis have been shown to share regulatory mechanisms in several tumors including WT.[4–6] Approaches that enable the assessment of both processes have been routinely used to uncover key molecular events that lead to cell transformation.

Nephrogenesis is a continuous process that involves different cell types, in variable proportions, the spatiotemporal localization of which has a role in the correct differentiation of the functional kidney. The triphasic WT histology resembles FK cells.[13] We previously analyzed the gene expression pattern of blastemal, stromal and epithelial components of WT separately and showed that blastema displays the most similar gene expression pattern of the initial stages of nephrogenesis, and that the Wnt signaling pathway is supposedly involved in the earliest events of WT onset.[6]

In the current study, a cell-resolution expression analysis was used for identifying disturbances in gene modulation of blastemal cell differentiation that can trigger a permissive condition for tumor development. We analyzed the expression modulation of Wnt and related signaling pathways genes in primordial blastemal WT cells and in four FK stages to identify conserved mechanisms in the earliest stages of kidney embryogenesis that recapitulate Wilms' tumorigenesis. The rationale behind this experimental design was to define alterations in gene expression modulation that are involved in the disruption of the differentiation process in the kidneys that lead to WT onset. To monitor gene expression in both processes, that is, tumorigenesis in humans and embryogenesis in mice, we used stringent parameters and generated reliable data from cross-species hybridization.

The signature of 18 Wnt and related signaling pathways genes displayed an expression pattern that was modulated during the differentiation of blastemal cells in nephrogenesis. Additionally the expression pattern of blastemal cells from the earliest stages of nefrogenesis in mice was recapitulated in blastemal cells from the WT in human. These results reinforced the importance of these genes in WT onset and also validated the approach used in this study.

Activation of the canonical Wnt signaling pathway has been continuously detected in WT verified by nuclear positivity of APC[6] and β-catenin.[8–10,14] In spite of the fact that no experimental evidence has been provided in this study to connect the 18 genes and activation of the canonical Wnt pathway, it is reasonable to suggest their involvement with this process in both nephrogenesis and WT.

Among the nine technically validated genes, *PAX2*, *IGF2*, *CRABP2*, *HDGF*, *SHPK*, *TESK1* and *WNT5B* were upregulated and *HIPK1* and *TIMP3* were downregulated at the mRNA level in WT blastemal cells than in DK glomerular cells.

PAX2 (located at 10q24) is a transcription factor that is expressed in FK nephrogenic structures and in WT, but is absent from the DK.[15] *PAX2* expression is suppressed by *WT1*, and both are essential for kidney development.[16] Inactivating *WT1* mutations have been observed in $\sim$10% of sporadic WT cases,[17] and germline mutations are associated with syndromes that include an increased WT incidence.[13] Consistent with these data, *PAX2* was similarly upregulated in this study at the mRNA level in WT as compared with the earliest FK developmental stages.

IGF2 (located at 11p15.5) is an embryonic growth factor and a member of the insulin family of polypeptides, with a role in kidney embryogenesis.[18] Under physiological conditions, the *IGF2* maternal allele is silenced by genomic imprinting, and the gene is expressed only by the paternal allele; however, WT exhibits a markedly increased expression relative to DK.[19,20] As expected, *IGF2* upregulation was detected in the earliest nephrogenesis stage, and this was recapitulated by WT both at the mRNA and at the protein levels.

WNT5B (located at 12p13.3) encodes a secreted Wnt signaling protein. CGH arrays of WTs have revealed a high level of gain of the *WNT5B* chromosomal locus,[21] which is in accordance with the transcriptional upregulation found in our study. However, no alteration at the protein level was observed in our results.

In addition, amplification of the chromosome region 1q22-q23.1, where *HDGF* and *CRABP2* are located, was also observed in WT samples,[21] and this is in agreement with the

Figure 3 Representative sections of immunohistochemical staining in Wilms tumor, fetal and differentiated kidneys. Proteins are identified in each block. Antibody specificity was determined by western blot (panels above graphics). Cell line and molecular weight are indicated. HEK293: human embryonic kidney cell line, SK-NEP-1: Wilms tumor cell line. Graphics: *Y* axis—protein quantification based on protein intensity values. *X* axis: Wilms tumor (right) and differentiated kidney (left) samples. A, D, G, J, M, P, S and V: representative samples of Wilms tumor. B, E, H, K, N, Q, T and X: representative samples of fetal kidneys. Fetal kidneys from thirteenth week human embryo: HDGF, IGF2, GRK7, WNT5B and TIMP3; fetal kidneys from seventeenth week human embryo: CRABP2 and FZD2, and; fetal kidneys from the twenty-fourth week human embryo: TESK1. C, F, I, L, O, R, U, Y representative samples of differentiated kidney, only cells from glomerulous were analyzed. WT: Wilms tumor; DK: differentiated kidney. (*) Represents differentially expressed genes with $P<0.05$. Black bars represent 100.1 or 100.3 μm as indicated in the green box

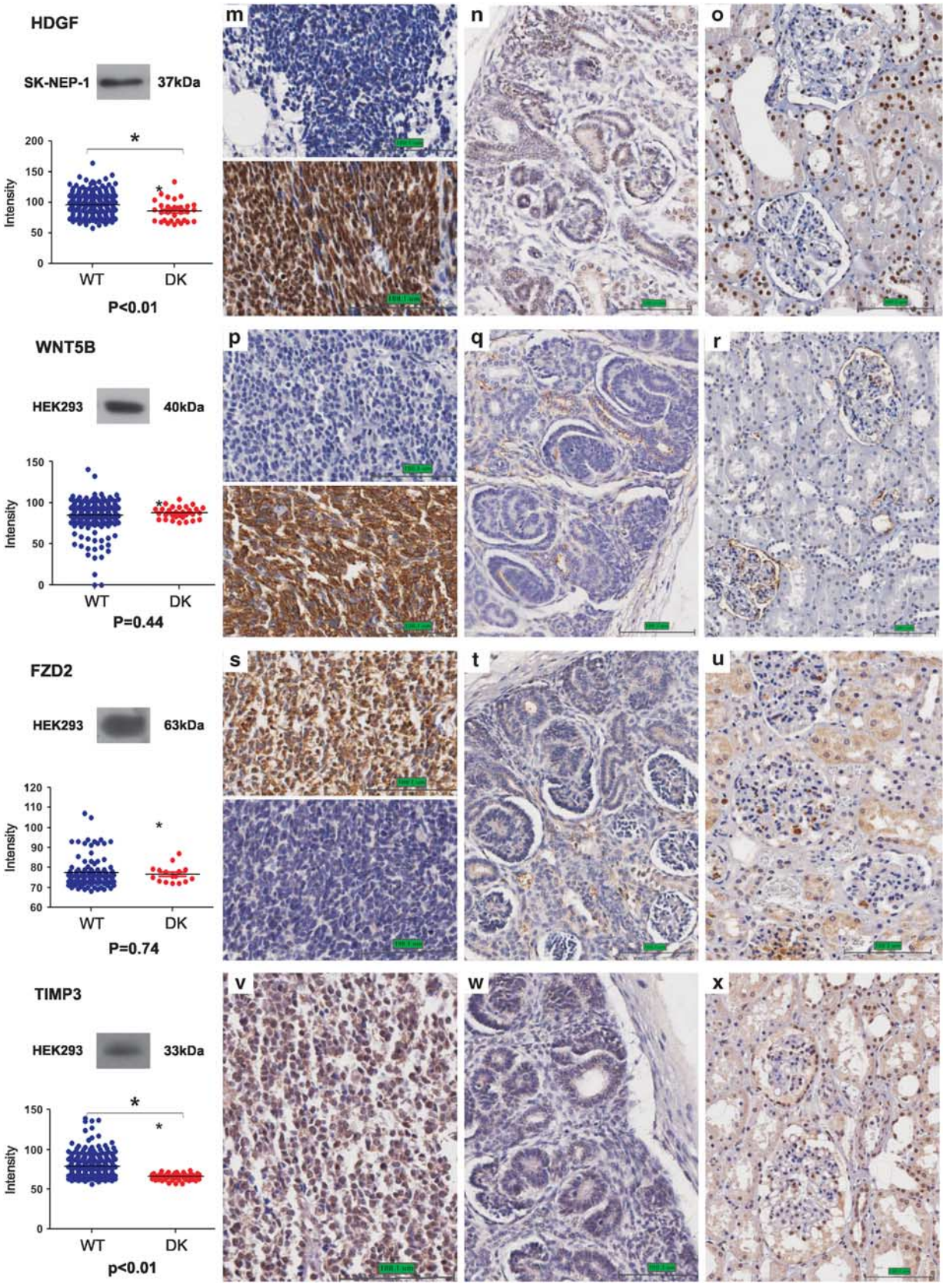

Figure 3 Continued

Table 3 Characterization of proteins expression in blastemal cells of WT, glomerulous cells of DK and in different stages of fetal kidneys

		WT		DK		
Protein	**Localization**	**Negative**	**Positive**	**Negative**	**Positive**	**Nephrogenesis**
CRABP2	Cytoplasm	6 (5.31%)	107 (94.69%)	18 (100%)	0 (0%)	Cytoplasm expression in cells going through MET
	Nucleus	7 (6.48%)	101 (93.52%)	17 (100%)	0 (0%)	
HDGF	Cytoplasm	62 (52.54%)	56 (47.56%)	12 (100%)	0 (0%)	Nuclear and cytoplasm expression in all stages of kidney differentiation
	Nucleus	59 (53.15%)	52 (46.85%)	18 (90%)	2 (10%)	
GRK7	Cytoplasm	1 (0.94%)	105 (99.06%)	11 (55%)	9 (45%)	Decreasing cytoplasm expression in cells during kidney differentiation
	Membrane	1 (0.86%)	116 (99.16%)	2 (9.09%)	20 (90.91%)	
TIMP3	Cytoplasm	15 (12.90%)	101 (87.10%)	26 (83.87%)	5 (16.13%)	Decreasing cytoplasmatic expression in blastemal cells during kidney differentiation
	Membrane	64 (57.66%)	47 (42.34%)	21 (100%)	0 (0%)	
WNT5B	Cytoplasm	112 (93.33%)	8 (6.67%)	10 (100%)	0 (0%)	Protein observed in the apical membrane of lumen cells that originate kidney structures
	Membrane	85 (75.22%)	28 (24.78%)	12 (60%)	8 (40%)	
FZD2	Membrane	69 (65.10%)	37 (34.90%)	3 (18.75%)	13 (81.25%)	Membrane expression in all stages of kidney cell differentiation
TESK1	Cytoplasm	4 (3.51%)	110 (96.49%)	20 (100%)	0 (0%)	Decreasing cytoplasm expression in cells during kidney differentiation
IGF2	Cytoplasm	16 (14.29%)	96 (85.71%)	10 (100%)	0 (0%)	Decreasing cytoplasmatic expression in cells during kidney differentiation

Abbreviation: MET, mesenchymal–epithelial transition

overexpression observed in our study. Our data also demonstrate slight HDGF overexpression at the protein level in blastemal cells than in DK glomerular cells, which reinforces the idea that HDFG is downregulated throughout organ differentiation.

In this study, *CRABP2* was upregulated both at the mRNA and at the protein level in WT blastemal cells than in cells from the cortex of DK samples in accordance with other studies in WT.[22,23] However, *CRABP2* downregulation has been observed in others tumor types including head and neck squamous cell carcinoma, in which a highly frequent hypermethylation rate was detected.[24] *CRABP2* encodes a cytosolic member of the retinoic acid-binding protein family involved in vitamin A metabolism, and moves to the nucleus upon binding of retinoic acid.[25] This cytosol-to-nuclear shuttling protein has an important role in embryogenesis. CRABP2 positivity was observed in a specific moment of kidney development when cells were going through MET after ureteric bud induction. This expression profile during nephrogenesis and the nuclear and cytoplasmatic positivity observed in the majority of WT blastemal components strongly suggests that CRABP2 mediates MET signaling of metanephric mesenchymal cells in the FK. Retinoic acid has been suggested for treatment of WT,[5,22,23] which indicates the necessity to carefully study *CRABP2* and retinoic acid in the context of WT and nephrogenesis. Little is known about the functional roles of retinoic acid and CRABP2 in kidney differentiation and WT tumorigenesis.

TIMP3 (located at 22q12.13) is a member of the *TIMP* gene family, which includes inhibitors of the matrix metalloproteinases and peptidases involved in degradation of the extracellular matrix. *TIMP3* is also an angiogenesis inhibitor that inhibits *VEGF* binding to *VEGFR2*.[26] We found decreased expression at the mRNA level and increased expression at the protein level in WT, suggesting a posttranscriptional mechanism of protein regulation for *TIMP3*.

GRK7 (located at 3q24) encodes a member of the guanine nucleotide-binding protein (G protein)-coupled receptor kinase subfamily of the serine threonine protein kinase family. *FZD2* (located at 17q21.1) encodes a seven-transmembrane domain protein involved in the signaling of both *CTNNB1*-dependent and *CTNNB1*-independent Wnt pathways. *FZD2* has been shown to be overexpressed in FKs and stem-like WT xenografts.[2] Accordingly, we observed upregulation at the mRNA level in WT and in the earliest kidney stages.

In addition, *WNT5B* and *FZD2* belong to the Wnt calcium signaling pathway, which has been recently shown to be involved with nephron formation through Wnt4 in mouse.[27] Interestingly, blastemal cells that express WNT5B also express FZD2 in FKs, although not all cells that express FZD2 express WNT5B (data not shown). Furthermore, glomerular DK cells and the epithelial component (the most differentiated WT component) express both proteins (data not shown), which supports the involvement of Wnt calcium signaling in blastemal cell differentiation, which may be perturbed in WT.

In spite of the fact that experimental delineation has favored identification of genes involved in the earliest event of WT onset that not necessarily have a role in WT progression, two genes, namely *IGF2* and *TESK1*, presented mRNA downregulation (with marginal statistical significance), showing a slightly association with relapse, which has been constantly investigated for better stratifying WT patients.[21,23,28,29] Further studies are necessary to definitively estimate the value of these genes for prognostic marker to be introduced in WT clinical routine.

It is possible that the utility of these gene expression data, in the context of molecular markers, will be in the application of therapeutic WT intervention because expression changes of these 18 genes seem to be in the earliest events in cell transformation. In addition, these alterations are present in the majority of tumor cells that increase their importance as molecular markers.

In summary, this study provides a clearer outline of the disruption of nephrogenesis and reveals new Wnt and related signaling pathway genes, which are highly likely to have crucial roles in WT biology.

Materials and Methods

Establishment of criteria for highly similar cDNA regions of orthologous genes. To identify highly similar regions between HM orthologous genes, 4608 partial human cDNA sequences immobilized on a custom cDNA platform[30] were BLASTed against mouse transcriptome databases (i.e. MGC, RefSeq and mRNAs/HTCs) using an *e*-value of -5 and a minimum alignment of 50% as parameters. This analysis revealed 1334 human sequences with matched mouse orthologous sequences. Visual inspection revealed an average similarity of 87%, which ranged from 79 to 98%, between sequences. These sequences were classified as highly conserved regions of HM orthologs (hcrHMs).

Reproducibility test of HM interspecies microarray hybridization. To determine the ideal hybridization conditions for HM interspecies hybridization, frozen human samples stored at $-140\,^{\circ}$C from three normal kidneys and three normal livers were obtained from the A.C. Camargo Hospital Tumor Tissue Biobank (São Paulo, Brazil), and total RNA pools were generated. A kidney and a liver were removed from an adult CD1 mouse, and total RNA was isolated using TRIzol (Invitrogen Life Technology, Carlsbad, CA, USA), according to the manufacturer's protocol.

A two-round RNA amplification was performed for all HM samples.[6] Labeled cDNA was generated by reverse transcription using 7 μg of amplified RNA (aRNA), random hexamer primers (Invitrogen), Cy3- or Cy5-labeled dCTP (Amersham Biosciences, Piscataway, NJ, USA) and SuperScript II (Invitrogen) according to the manufacturer's protocol. Dye-swap experiments were performed for intraspecific (i.e. human samples and a human cDNA platform) and interspecific (i.e. mouse samples and a human cDNA platform) hybridizations for dye bias control. Prehybridization and hybridization were performed as described previously.[6] After background subtraction, quantified signals were log transformed, and a nonlinear normalization (Lowess) was applied to correct experimental bias within each array.

Dye-swap hybridizations were performed in triplicate for HM samples, and generated data were used for mathematical and statistical analyses. The reproducibility of signal intensities was evaluated for the 1334 hcrHMs by Pearson's correlations between replicates and Levene's tests among triplicates.[31] For the latter, spot signal intensity values from HM triplicates were plotted to calculate the S.D. and signal intensity variance. Variance values from the intraspecific hybridizations were used as a standard and compared with those from the interspecific hybridizations.

Construction of a cDNA platform for HM interspecies microarray hybridization. To define the hcrHMs of 326 genes representative of Wnt and related signaling pathways (Supplementary File 1), human FASTA sequences were BLASTed against mouse transcriptome databases (i.e. MGC, RefSeq and mRNAsHTCs) using described parameters ($>50\%$ identity and an *e*-value of -5).

Primers were designed to flank the hcrHMs of 101 genes, and RT-PCR was performed using cDNAs converted from a pool of total RNA from 15 human cell lines as described previously.[32] The amplicons were extracted from 1% agarose gel and cloned using the InsTAclone kit (Fermentas Life Science , Hanover, MD, USA). For 225 genes, a cDNA clone that covered at least 80% of the respective hcrHMs was retrieved from our cDNA bank from the Human Cancer Genome Project.[33,34] All cDNAs were amplified using universal reverse or forward primers, sequenced in a 3130xl Capillary Genetic Analyzer (Applied Biosystems, Foster City, CA, USA) to confirm cDNAs' identities, purified with G50 resin and arrayed onto glass slides using a Flexys robot (Genomic Solutions, Ann Arbor, MI, USA).

The cDNA platform comprised 2352 spots and included 326 hcrHMs, 1384 additional human cDNA sequences, 496 negative controls (DMSO) and 48 positive controls (the *Q* gene from λ-phage).

Tissue sample and cell laser microdissection. In total, 59 frozen samples with favorable WT histology, including a predominance of blastemal component histology, were received from COG (Children's Oncology Group). Sections of 5μm from fresh frozen tumor blocks were excised onto glass slides and stained with hematoxylin and eosin for review by a pathologist (FAS).

The PixCell II LCM system (Arcturus Engineering, Mountain View, CA, USA) was used for laser microdissection of 24 blastemal cells. Samples were mounted onto glass slides and stained with 100 μl of nuclear fast red (Certistain; Merck) for visualization using CapSure Macro LCM Caps (Arcturus Engineering). These samples were used for cDNA microarrays and technical validation experiments. For an independent sample group, 35 out of the 59 samples were scalpel dissected to enrich for blastemal cells (a minimum of 80%) for the RT-qPCR validation steps. In all, 17 histologically normal DKs were retrieved from A.C. Camargo Hospital Tumor Tissue Biobank. Glomerular cells from 4 out of 17 kidneys were laser microdissected and used for the cDNA microarray experiments. The renal cortices from 13 out of 17 kidneys were dissected for the RT-qPCR validation steps. On average, 2000 cells were captured for laser-microdissected samples (Supplementary Figure 2).

The kidneys from CD1 strain mice were isolated from embryos (E) and postnatal animals (P) at ages E15.5, E17.5, P1.5 and P7.5. Three animals from each age were independently processed and used as replicates, except for E15.5, which was represented by one embryo. Dissected tissues were immediately frozen in liquid nitrogen and treated as described above. Cells from metanephric mesenchyme, metanephric blastema and fully differentiated glomerulus were laser microdissected, considering the proportions of each cell type in each mouse stage, using CapSure HS LCM Caps (Arcturus Engineering). On average, 400 cells were captured.

Two pathologists (FAS and RC) supervised all dissection procedures. This study was in accordance with the principles of the Declaration of Helsinki and was approved by the A.C. Camargo Hospital Ethics Committee under number CEP 764/06 for human samples. All animal experiments were also conducted according to the guidelines of the A.C. Camargo Hospital Animal Ethics Committee under the number CEUA 006/06.

RNA extraction and amplification. RNA from laser-microdissected samples was purified using the PicoPure RNA isolation kit (Arcturus Engineering) and treated using an RNase-Free DNase set (Qiagen, Germantown, MD, USA). Total RNA from scalpel-dissected samples was extracted using TRIzol (Invitrogen). To generate aRNA, we used the RiboAmp RNA amplification kit, and the RiboAmp HS plus kit (Arcturus Engineering) for HM samples, respectively. RNA quantity and purity were determined by spectrophotometry NanoDrop ND-1000 (Thermo Scientific, Wilmington, DE, USA). Total RNA integrity was analyzed by Agilent Bioanalyzer 2100 (Agilent Technologies, Palo Alto, CA, USA) and only those with an OD $260/280 \geq 1.8$ and an RIN >5.0 were used for microarray and RT-qPCR experiments.

cDNA microarray experiments. A pool of RNAs[32] was used as the reference sample. Labeled cDNA was generated using 7 and 4 μg of aRNA from the test and reference samples, respectively, random hexamer primers (Invitrogen), Cy3- or Cy5-labeled dCTP (Amersham Biosciences) and SuperScript III (Invitrogen) for competitive hybridization to the cDNA platform. Dye swapping was performed for each sample to control for dye bias, and this was used as a replicate.

For mouse samples, dye-swapping experiments were conducted in triplicate for animals aged E17.5, P1.5 and P7.5 and for one replicate of E15.5. Data acquisition and normalization were performed as described previously.[6] The microarray data files were deposited in the GEO/NCBI public database identified as GSE25965 (http://www.ncbi.nlm.nih.gov/geo/query/acc.cgi?acc = GSE25965).

RT-qPCR. To validate the differentially expressed genes from microarray experiments, the initial sample set was evaluated using RT-qPCR, which is referred to here as technical validation. cDNA was synthesized from 2 μg of aRNA using SuperScript III (Invitrogen) and random hexamer primers. For an independent sample set, which is referred to here as biological validation, cDNA was synthesized from 2 μg of DNase-treated total RNA using IMPROM II (Promega, Madison, WI, USA) and oligo-dT(24) primers, according to the manufacturer's protocol. RT-qPCR was performed in the ABI Prism 7900 sequence detection system (Applied Biosystems) using SYBR Green PCR Master Mix (Applied Biosystems) in a 20 μl total volume. All reactions were performed in duplicate, and no-template reactions were used as a negative control. The amplification efficiency of each primer pair was calculated using standard curve dilutions[35] (Table 4). *ACTB* and *GAPDH* were

Table 4 Characteristics of primers used for qRT-PCR.

Genes	Forward primer	Reverse primer	Amplified fragment (pb)	Amplification efficiency (%)
ACTB	CAGGATGCAGAAGGAG	CTGCTGGAAGGTGGAC	130	100
GAPDH	CTTTGTCAAGCTCATTTCC	CTTACTCCTTGGAGGCC	92	100
SHPK	CCTTGGGTGATTTACAG	GAATCCTGAAGGCATGG	110	100
CRABP2	GGTGAAATGGGAGAGTG	CGTAGACCCTGGTGCAC	152	100
FRZB	GTGGAAGGATCGACTCG	GAGTTCCTGCCAGACTTC	124	120
HDGF	GCTACCAAGGAAGATGCTG	GACAGCAGCAGGAACAGG	100	100
HIPK1	GACCAGTGCAGCACAAC	GCTGGGTTGCTGCTTC	87	106
IGF2	CTGGAGACGTACTGTGC	GCTTCCAGGTGTCATATTG	114	100
ITPR3	CAACTCCACCATGAAGCTG	GTTCTGGACATCCACAAAGC	61	106
PAX2	CACTCTGCCTGGTTACC	GTGGCTGTACGGGTTG	115	100
PIK3CA	GTGATTAGTAAAGGAGCCC	GAGATTGGCATGCTGTCG	105	96
TESK1	CCTTCACCGAAATTACCCA	GGAAGCGTGGCAGAGG	130	100
TIMP3	CTGAACTATCGGTATCACC	CTCGTTCTTGGAAGTCAC	84	100
WNT5B	CTCATGAACCTGCACAAC	CTACATGAGCCGGACAC	95	100

Table 5 Antibodies, retrieval characteristics and evaluated localization of each protein with the correspondent limit intensity used for defining positive and negative samples

Protein	Antibody	Title	Dilution	Antigen retrieval	Localization	Cutoff
CRABP2	Mouse polyclonal anti-CRABP2	MAB5488, Chemicon (Temecula, CA, USA)	1 : 2000	Citrate, pH 6.0	cytoplasm nucleus	81 96
FZD2	Rabbit polyclonal anti-FZD2	AB26396, Abcam (Temecula, CA, USA)	1 : 2000	EDTA-TRIS, pH 9.0	membrane	73
HDGF	Monoclonal anti-HDGF	AB58644, Abcam	1 : 100	Citrate, pH 6.0	cytoplasm nucleus	80 110
GRK7	Rabbit polyclonal anti-GRK7	AP7731b, Abgent (San Diego, CA, USA)	1 : 100	Citrate, pH 6.0	cytoplasm membrane	85 91
TIMP3	Mouse monoclonal anti-TIMP3	AB49670, Abcam	1 : 100	EDTA-TRIS, pH 8.0	cytoplasm membrane	70 69
WNT5B	Rabbit polyclonal anti-WNT5B	LS-A8730, Lifespan (Seattle, WA, USA)	1 : 400	Citrate, pH 6.0	cytoplasm membrane	103 88
TESK1	Rabbit polyclonal anti-TESK1	AP7820b, Abgent	1 : 200	Citrate, pH 6.0	cytoplasm	68
IGF2	Rabbit polyclonal anti-IGF2	LS-C7512, Lifespan	1 : 2000	Citrate, pH 6.0	cytoplasm	75

selected as the most stable control genes from four endogenous genes tested (*GAPDH*, *ACTB*, *HPRT1* and *BCR*) using the geNorm algorithm.[36]

TMA construction and immunohistochemistry assays. Formalin-fixed, paraffin-embedded (FFPE) WT and kidney specimens from 145 and 20 patients, respectively, were obtained from the Pathology Department of the A.C. Camargo Hospital. For tissue microarray (TMA) construction, hematoxylin and eosin sections were analyzed, and a representative area of the tumor blastemal component and the kidney cortex region was marked on the slide. Selected areas from each sample were arrayed once with a 1.0-mm diameter core that was spaced 0.2 mm apart using a Tissue Microarrayer (Beecher Instruments, Silver Spring, MD, USA).

Additional slides from 19 FFPE postmortem human fetuses at 13 to 24 weeks (i.e. 13, 17, 18, 19, 20, 21, 22 and 24 weeks) of gestation were obtained from the University of São Paulo Medical School in accordance with the authorization of their ethics committee.

Slides were deparaffinized, rehydrated and then subjected to antigen retrieval. The antigen retrieval method details and primary antibody clones are described in Table 5. Sections were incubated in 3% aqueous hydrogen peroxide for 15 min to quench endogenous peroxidase activity and treated with serum-free protein block (Dako, Copenhagen, Denmark) for 20 min at room temperature to suppress nonspecific binding. Immunohistochemical reactions were performed using a polymer technique (Dako). The slides were incubated with the biotinylated secondary antibody from the LSAB + peroxidase kit (Dako), followed by incubation with streptavidin–horseradish peroxidase (HRP) (Dako) and were then counter-stained with hematoxylin.

Western blot analysis was performed to check the specificity of antibodies used in IHC assay. HEK293 (CRL-1573) and SK-NEP-1 (HTB-48) cell lines (American Type Culture Collection, ATCC, Manassas, VA, USA) were maintained in a humidified incubator at 37 °C in the presence of 5% CO_2. The HEK293 cell line was cultured in DMEM medium (Gibco, Carlsbad, CA, USA) supplemented with 10% FBS and 1% L-glutamine, and SK-NEP-1 cells were maintained in McCoy's 5A medium (Gibco) supplemented with 15% FBS and 1% L-glutamine. Total protein were extract from subconfluent culture cells with cold RIPA buffer (50 mM Tris-HCl (pH 8.0), 150 mM NaCl, 1% Nonidet P-40, 0.5% sodium deoxicolate, 0.1% SDS and 1 × complete, mini protease inhibitor cocktail (Roche, Mannheim, Germany) and 1 × PhosSTOP phosphatase inhibitor cocktail (Roche)) and western blot assays were performed as described previously.[37] Proteins were detected using rabbit polyclonal anti-GRK7 (1 : 500), anti-WNT5B (1 : 100), anti-TIMP3 (1 μg/ml), anti-FZD2 (1 μg/ml), anti-IGF2 (1 : 1000), anti-TESK1 (1 : 500) and mouse monoclonal anti-CRABP2 (1 : 250) and anti-HDGF (1 : 500) antibodies. Signals were detected using ECL HRP-conjugated immunoglobulin G whole antibodies (1 : 2000, GE Healthcare, Little Chalfont, UK).

Protein localization was determined for the nucleus, membrane and cytoplasm. Immunohistochemical expression was quantitatively analyzed using the Automated Cellular Imaging System III (ACIS) (Dako), which detects hue, saturation and luminosity levels and converts these signals into a numerical density measurement that ranges from 0 to 256. Each cell compartment (nucleus, membrane and cytoplasm) evaluated using the ACIS equipment requires an independent slide scanning. Therefore, the number of high-quality images of each protein able to cell recognition and intensity measurement could vary.

For each of the eight proteins analyzed, the pathologist established a limit intensity value by visual evaluation, and this was considered the cutoff value (Table 5). Samples with intensity values lower than the cutoff and/or with $<10\%$ of cells labeled were considered to be negatively stained. Accordingly, samples with intensity values higher than the cutoff intensity were considered to be positively stained. For DKs, only glomerular cells were used for this analysis because of a high level of nonspecific labeling of tubule cells.

Mathematical and statistical analysis. Student's *t*-test was used to identify differentially expressed genes between WT and DK in the cDNA microarray experiments. The differentially expressed genes were annotated in the Gene Ontology Database biological process categories and organized in a hierarchical manner through automated EASE gene function analysis.[38] To characterize gene expression modulation during the four stages of nephrogenesis, the average signal

intensity among triplicates of dye-swap microarray experiments was plotted in graphs to create a curve to report the expression tendency. Pearson's correlation and complete linkage were used for nonsupervised hierarchical clustering, and reliability was assessed by bootstrapping using TMEV version 4.6.

For RT-qPCR experiments, relative fold changes were calculated considering primer efficiency, and genes were considered to be differentially expressed when they reached the previously described criteria of a P-value < 0.05 by the t-test and a fold change ≥ 3 to avoid artifactual results in the relative gene expression data, as recommended previously.[39]

Membrane, cytoplasm and nucleus density measurements from immunohistochemistry assays were plotted in a graph, and Student's t-test was applied to find significant differences in labeling between WT blastemal cells and DK glomerular cells ($P \leq 0.05$).

Conflict of Interest

The authors declare no conflict of interest.

Acknowledgements. We thank COG and Biobank of A.C. Camargo Hospital for providing WT tissue samples and FAPESP for funding this work. We also thank technicians from the Department of Anatomic Pathology and Ricardo R Brentani for critical revision of the manuscript. FAPESP is a non-profit foundation and funds science at São Paulo state in Brazil. This work was supported by FAPESP 06/00054-0 and 2010/00223-1. MM, APT and FSP were supported by fellowships from FAPESP.

Authors apologize for the omission of important citations by limited number of references recommended by the journal

1. Schedl A. Renal abnormalities and their developmental origin. *Nat Rev Genet* 2007; **8**: 791–802.
2. Dekel B, Metsuyanim S, Schmidt-Ott KM, Fridman E, Jacob-Hirsch J, Simon A *et al.* Multiple imprinted and stemness genes provide a link between normal and tumor progenitor cells of the developing human kidney. *Cancer Res* 2006; **66**: 6040–6049.
3. Metsuyanim S, Harari-Steinberg O, Buzhor E, Omer D, Pode-Shakked N, Ben-Hur H *et al.* Expression of stem cell markers in the human fetal kidney. *PLoS One* 2009; **4**: e6709.
4. Li CM, Guo M, Borczuk A, Powell CA, Wei M, Thaker HM *et al.* Gene expression in Wilms' tumor mimics the earliest committed stage in the metanephric mesenchymal-epithelial transition. *Am J Pathol* 2002; **160**: 2181–2190.
5. Li W, Kessler P, Williams BR. Transcript profiling of Wilms tumors reveals connections to kidney morphogenesis and expression patterns associated with anaplasia. *Oncogene* 2005; **24**: 457–468.
6. Maschietto M, de Camargo B, Brentani H, Grundy P, Sredni S, Torres C *et al.* Molecular profiling of isolated histological components of Wilms tumor implicates a common role for the Wnt signaling pathway in kidney and tumor development. *Oncology* 2008; **75**: 81–91.
7. Klaus A, Birchmeier W. Wnt signalling and its impact on development and cancer. *Nat Rev Cancer* 2008; **8**: 387–398.
8. Sredni S, Maschieto M, de Camargo B, Soares F. Myogenesis in Wilms tunors. *Pediatric and Developmental Pathology* 2004; **7**: 668–669.
9. Fukuzawa R, Anaka MR, Weeks RJ, Morison IM, Reeve AE. Canonical WNT signalling determines lineage specificity in Wilms tumour. *Oncogene* 2009; **28**: 1063–1075.
10. Fukuzawa R, Heathcott RW, Sano M, Morison IM, Yun K, Reeve AE. Myogenesis in Wilms' tumors is associated with mutations of the WT1 gene and activation of Bcl-2 and the Wnt signaling pathway. *Pediatr Dev Pathol* 2004; **7**: 125–137.
11. Strutt D. Frizzled signalling and cell polarisation in Drosophila and vertebrates. *Development* 2003; **130**: 4501–4513.
12. Tamimi Y, Ekuere U, Laughton N, Grundy P. WNT5A is regulated by PAX2 and may be involved in blastemal predominant Wilms tumorigenesis. *Neoplasia* 2008; **10**: 1470–1480.
13. Rivera MN, Haber DA. Wilms' tumour: connecting tumorigenesis and organ development in the kidney. *Nat Rev Cancer* 2005; **5**: 699–712.
14. Koesters R, Niggli F, von Knebel Doeberitz M, Stallmach T. Nuclear accumulation of beta-catenin protein in Wilms' tumours. *J Pathol* 2003; **199**: 68–76.
15. Dressler GR, Douglass EC. Pax-2 is a DNA-binding protein expressed in embryonic kidney and Wilms tumor. *Proc Natl Acad Sci USA* 1992; **89**: 1179–1183.
16. Discenza MT, He S, Lee TH, Chu LL, Bolon B, Goodyer P *et al.* WT1 is a modifier of the Pax2 mutant phenotype: cooperation and interaction between WT1 and Pax2. *Oncogene* 2003; **22**: 8145–8155.
17. Little SE, Hanks SP, King-Underwood L, Jones C, Rapley EA, Rahman N *et al.* Frequency and heritability of WT1 mutations in nonsyndromic Wilms' tumor patients: a UK Children's Cancer Study Group Study. *J Clin Oncol* 2004; **22**: 4140–4146.
18. Scott J, Cowell J, Robertson ME, Priestley LM, Wadey R, Hopkins B *et al.* Insulin-like growth factor-II gene expression in Wilms' tumour and embryonic tissues. *Nature* 1985; **317**: 260–262.
19. Ogawa O, Eccles MR, Szeto J, McNoe LA, Yun K, Maw MA *et al.* Relaxation of insulin-like growth factor II gene imprinting implicated in Wilms' tumour. *Nature* 1993; **362**: 749–751.
20. Bjornsson HT, Brown LJ, Fallin MD, Rongione MA, Bibikova M, Wickham E *et al.* Epigenetic specificity of loss of imprinting of the IGF2 gene in Wilms tumors. *J Natl Cancer Inst* 2007; **99**: 1270–1273.
21. Natrajan R, Williams RD, Hing SN, Mackay A, Reis-Filho JS, Fenwick K *et al.* Array CGH profiling of favourable histology Wilms tumours reveals novel gains and losses associated with relapse. *J Pathol* 2006; **210**: 49–58.
22. Gupta A, Kessler P, Rawwas J, Williams BR. Regulation of CRABP-II expression by MycN in Wilms tumor. *Exp Cell Res* 2008; **314**: 3663–3668.
23. Li W, Kessler P, Yeger H, Alami J, Reeve AE, Heathcott R *et al.* A gene expression signature for relapse of primary Wilms tumors. *Cancer Res* 2005; **65**: 2592–2601.
24. Calmon MF, Rodrigues RV, Kaneto CM, Moura RP, Silva SD, Mota LD *et al.* Epigenetic silencing of CRABP2 and MX1 in head and neck tumors. *Neoplasia* 2009; **11**: 1329–1339.
25. Sessler RJ, Noy N. A ligand-activated nuclear localization signal in cellular retinoic acid binding protein-II. *Mol Cell* 2005; **18**: 343–353.
26. Qi JH, Ebrahem Q, Moore N, Murphy G, Claesson-Welsh L, Bond M *et al.* A novel function for tissue inhibitor of metalloproteinases-3 (TIMP3): inhibition of angiogenesis by blockage of VEGF binding to VEGF receptor-2. *Nat Med* 2003; **9**: 407–415.
27. Tanigawa S, Wang H, Yang Y, Sharma N, Tarasova N, Ajima R *et al.* Wnt4 induces nephronic tubules in metanephric mesenchyme by a non-canonical mechanism. *Dev Biol* 2011; **352**: 58–69.
28. Williams RD, Hing SN, Greer BT, Whiteford CC, Wei JS, Natrajan R *et al.* Prognostic classification of relapsing favorable histology Wilms tumor using cDNA microarray expression profiling and support vector machines. *Genes Chromosomes Cancer* 2004; **41**: 65–79.
29. Maschietto M, Piccoli FS, Costa CM, Camargo LP, Neves JI, Grundy PE *et al.* Gene expression analysis of blastemal component reveals genes associated with relapse mechanism in Wilms tumour. *Eur J Cancer* 2011; e-pub ahead of print 22 June 2011.
30. Brentani RR, Carraro DM, Verjovski-Almeida S, Reis EM, Neves EJ, de Souza SJ *et al.* Gene expression arrays in cancer research: methods and applications. *Crit Rev Oncol Hematol* 2005; **54**: 95–105.
31. Carroll R, Schneider H. A note on Levene's tests for equality of variances. *Stat Probab Lett* 1995; **3**: 191–194.
32. Mello BP, Abrantes EF, Torres CH, Machado-Lima A, Fonseca RaS, Carraro DM *et al.* No-match ORESTES explored as tumor markers. *Nucleic Acids Res* 2009; **37**: 2607–2617.
33. Brentani H, Caballero OL, Camargo AA, da Silva AM, da Silva WA, Dias Neto E *et al.* The generation and utilization of a cancer-oriented representation of the human transcriptome by using expressed sequence tags. *Proc Natl Acad Sci USA* 2003; **100**: 13418–13423.
34. Camargo AA, Samaia HP, Dias-Neto E, Simão DF, Migotto IA, Briones MR *et al.* The contribution of 700,000 ORF sequence tags to the definition of the human transcriptome. *Proc Natl Acad Sci USA* 2001; **98**: 12103–12108.
35. Pfaffl MW. A new mathematical model for relative quantification in real-time RT-PCR. *Nucleic Acids Res* 2001; **29**: e45.
36. Vandesompele J, De Preter K, Pattyn F, Poppe B, Van Roy N, De Paepe A *et al.* Accurate normalization of real-time quantitative RT-PCR data by geometric averaging of multiple internal control genes. *Genome Biol* 2002; **3**: RESEARCH0034.
37. Ricca TI, Liang G, Suenaga AP, Han SW, Jones PA, Jasiulionis MG. Tissue inhibitor of metalloproteinase 1 expression associated with gene demethylation confers anoikis resistance in early phases of melanocyte malignant transformation. *Transl Oncol* 2009; **2**: 329–340.
38. Dennis G, Sherman BT, Hosack DA, Yang J, Gao W, Lane HC *et al.* DAVID: database for annotation, visualization, and integrated discovery. *Genome Biol* 2003; **4**: P3.
39. Ferreira E, Maschietto M, Silva S, Brentani H, Carraro D. Evaluation of quantitative RT-PCR using nonamplified and amplified RNA. *Diagn Mol Pathol* 2010; **19**: 45–53.

SOME RIGHTS RESERVED

Cell Death and Disease **is an open-access journal published by** ***Nature Publishing Group.*** **This work is licensed under the Creative Commons Attribution-Noncommercial-No Derivative Works 3.0 Unported License. To view a copy of this license, visit http://creativecommons.org/licenses/by-nc-nd/3.0/**

Supplementary Information accompanies the paper on Cell Death and Disease website (http://www.nature.com/cddis)